The role of angular momentum in collision-induced vibration–rotation relaxation in polyatomics

Anthony J. McCaffery and Mark A. Osborne
Department of Chemistry, University of Sussex, Brighton BN19QJ, United Kingdom

Richard J. Marsh
Department of Physics, University College, Gower St., London WC1E6BT

Warren D. Lawrance and Eric R. Waclawik
School of Chemistry, Physics and Earth Sciences, Flinders University, G.P.O. Box 2100, Adelaide, South Australia 5001, Australia

(Received 27 October 2003; accepted 13 April 2004)

Vibrational relaxation of the 6^1 level of $S_1(^1B_{2u})$ benzene is analyzed using the angular momentum model of inelastic processes. Momentum–(rotational) angular momentum diagrams illustrate energetic and angular momentum constraints on the disposal of released energy and the effect of collision partner on resultant benzene rotational excitation. A kinematic ''equivalent rotor'' model is introduced that allows quantitative prediction of rotational distributions from inelastic collisions in polyatomic molecules. The method was tested by predicting *K*-state distributions in glyoxal–Ne as well as *J*-state distributions in rotationally inelastic acetylene–He collisions before being used to predict *J* and *K* distributions from vibrational relaxation of 6^1 benzene by H_2, D_2, and CH_4. Diagrammatic methods and calculations illustrate changes resulting from simultaneous collision partner excitation, a particularly effective mechanism in p-H_2 where some 70% of the available $6^1 \rightarrow 0^0$ energy may be disposed into $0 \rightarrow 2$ rotation. These results support the explanation for branching ratios in $6^1 \rightarrow 0^0$ relaxation given by Waclawik and Lawrance and the absence of this pathway for monatomic partners. Collision-induced vibrational relaxation in molecules represents competition between the magnitude of the energy gap of a potential transition and the ability of the colliding species to generate the angular momentum (rotational and orbital) needed for the transition to proceed. Transition probability falls rapidly as ΔJ increases and for a given molecule–collision partner pair will provide a limit to the gap that may be bridged. Energy constraints increase as collision partner mass increases, an effect that is amplified when $J_i > 0$. Large energy gaps are most effectively bridged using light collision partners. For efficient vibrational relaxation in polyatomics an additional requirement is that the molecular motion of the mode must be capable of generating molecular rotation on contact with the collision partner in order to meet the angular momentum requirements. We postulate that this may account for some of the striking propensities that characterize polyatomic energy transfer. © *2004 American Institute of Physics.*
[DOI: 10.1063/1.1758696]

I. INTRODUCTION

Collision-induced vibration and rotation state change in polyatomic molecules has been much less studied than the corresponding processes in diatomics.[1] However the number of additional excitation and relaxation routes in polyatomic molecules brings new possibilities, raising fundamental questions concerning the dynamical behavior of molecules.[2–6] Parmenter,[2] Rice[3] among others have drawn attention to the extraordinarily selective nature of vibrational transfer (VT) in large molecules. Waclawik and Lawrance[4,5] demonstrated that angular momentum (AM) factors exercise a controlling influence on VT in excited benzene. Alwahabi *et al.*[6] showed that rotational transfer (RT) rate constants in NH_2 fall exponentially with transferred AM and are unrelated to the amount of energy transferred. These two experiments indicate that minimum *energy change* may be less important than minimum *angular momentum change* in collisions involving polyatomics. Molecular rotational AM appears to play a central role in most forms of energy exchange involving diatomic molecules.[7,8] A simple, effective approach to predicting the state-to-state outcome of collisions consists of direct calculation of the probability of linear-to-(rotational) angular momentum conversion (orbital-to-rotational in the case of reactive collisions).[7,8] We explore this proposal here in the context of polyatomic collisions with particular reference to $6^1 \rightarrow 0^0$ transfer in benzene.

Collisions involving large molecules pose considerable problems to the theorist, particularly when the fate of molecular rotations is of interest. Early models of VT based on the collinear collision geometry[3,9] did not include rotational state change. Calculation of VT propensities using quantum scattering methods become intractable when large numbers of rotational channels are open and consequently the effect of rotations on polyatomic VT has not been widely explored. The vibrationally close-couple–infinte order sudden (VCC-IOS) technique introduced by Clary[10] and often used to pre-

dict vibration–rotation transfer (VRT) probabilities in large molecules effectively freezes rotations throughout the collision. In diatomic molecules the efficient disposal of angular momentum is a critical factor in determining cross-sections for pure RT, VRT,[11] electronic energy transfer,[12] vibrational predissociation of van der Waals molecules,[13] and atom–diatomic molecule exchange reactions.[14] Direct calculation of the probability of linear-to-angular momentum conversion is fast and yields accurate results.[7,8] Extension to the polyatomic case however is quite challenging. Rotation may occur about more than one molecular axis and collisions cause transitions within or between the discrete energy levels that arise from rotations about these axes. A dynamical AM model relates RT probabilities to the AM gap both within and across (J,K_a,K_c) levels.[15] However, it is often found that one of either the *J*- or *K*-changing processes dominates, particularly if the molecules are actual or near symmetric tops. A simpler theoretical approach limited either to *J*- or to *K*-changing transitions might represent a useful contribution to this important topic.

Experiments on collision-induced $6^1 \rightarrow 0^0$ vibrational relaxation of the S_1 level of benzene by monatomic and polyatomic collision partners[4,5] showed the nuclear dynamics of momentum disposal to be the controlling factor in this VRT process. Parmenter and co-workers,[16] in a series of crossed beam experiments, convincingly demonstrated the central role played by kinematic factors in RT and VRT involving glyoxal. These results suggest that the AM model of inelastic processes,[7,8] developed initially for diatomics, might be useful in the analysis of collision-induced transfer in larger molecules. The approach has both qualitative and quantitative elements. Graphical techniques in which energy and AM conservation relationships are plotted as velocity–angular momentum $(v_r - \Delta J)$ diagrams provide qualitative predictions of rotational distribution shapes and peak values. Calculations using a hard shape representation of the molecule and the physics of momentum exchange reproduce experimental data with high accuracy.

A quantitative model that would predict simultaneous *J*- and *K*-changing processes is not feasible at present due to the difficulty of devising a generalized hard shape representation for polyatomics. Here we adopt a strategy having more limited aims. We begin by demonstrating that $v_r - \Delta J$ diagrams for the $6^1 \rightarrow 0^0$ VRT process in benzene give insight into the nuclear dynamics of the event and the manner in which di- or polyatomic collision partners may influence disposal of energy and angular momentum. These show how VRT probabilities change when di- and polyatomic molecules are involved. These follow explanations given earlier,[5,6] but arguments are quantified and demonstrate an emerging pattern that stresses the importance of AM in determining collision outcomes. $v_r - \Delta J$ plots may be constructed for *J*- and *K*-changing collisions separately and (J,K) changing is readily incorporated if data are available. We next introduce a simple ''equivalent rotor'' model that allows quantitative calculations to be made of final *J or K* distributions following RT and VRT. The basis is a rigid ellipsoid having the same moment of inertia and major axis length as that of the molecule along the inertial axis giving rise to particular *J*- or *K*-changing transition. The model is described in Sec. III and predictions for *J*- or *K*-changing processes are compared to experiment in Sec. IV.

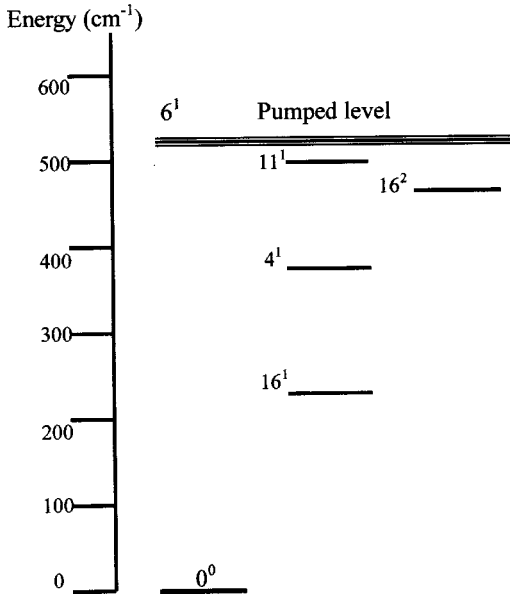

FIG. 1. Lowest vibrational levels of S_1 benzene.

II. QUALITATIVE ANALYSIS OF $6^1 \rightarrow 0^0$ VIBRATIONAL RELAXATION IN S_1 BENZENE

Studies of collision-induced $6^1 \rightarrow 0^0$ vibrational relaxation of S_1 benzene with a wide range of mono- and polyatomic collision partners have revealed intriguing propensities.[4,5] Analysis indicates that relaxation is controlled by factors related to the disposal of angular momentum and is unrelated to detailed features of the intermolecular potential. These conclusions were drawn from experiments in the absence of full resolution of rotational features.[4] More recent high-resolution data[5] reveal the rotational structure associated with the $6^1 \rightarrow 0^0$ transition when H_2, D_2, and CH_4 are the collision partners. This structure is partner dependent, being particularly extensive with methane. Possible vibrational state destinations from 6^1 may be seen in the $S_1(^1B_{2u})$ level diagram (Fig. 1). We consider only those events that populate the 0^0 vibrational level as well as the reasons for those that do not. A brief summary of the experimental findings is as follows. Monatomic collision partners are *unable* to cause transitions $6^1 \rightarrow 0^0$ under the conditions of the experiment.[4] Transitions occur to other, lower energy gap, vibrational levels with the rare gases however and here the branching ratios appear uniform for He, Ne, Ar, and Kr. This may be deceptive as one of the transfer channels refers to two destination levels that cannot be separated spectroscopically. In these, rotational excitation increases with collision partner mass. When di- and polyatomic collision partners are introduced the most striking new feature is that transitions to the 0^0 level of benzene are seen,[4] their intensity following the order $H_2 > D_2 > CH_4 > c\text{-}C_3H_6 > C_2H_2 > N_2$. Furthermore, the extent of the 0^0 rotational structure varies markedly with collision partner. This

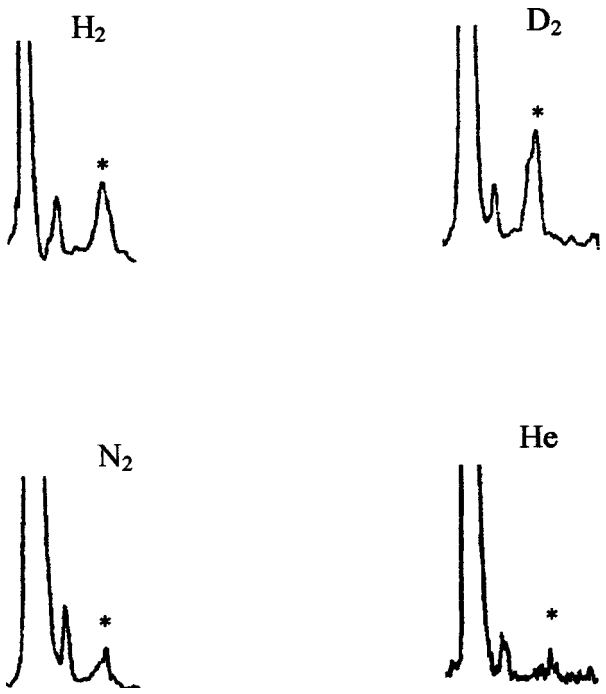

FIG. 2. Dispersed fluorescence in the $6^1 \rightarrow 0^0$ region following excitation of 6^1 in benzene for collision partners H_2, D_2, N_2, and He. Asterisks identify the transitions to 0^0.

is evident in Fig. 2 where the 0^0 features resulting from deactivation by a range of collision partners are displayed.

The first step in the analysis of benzene VRT consists of close examination of relevant $v_r - \Delta J$ diagrams for this transition since these may be used to estimate the shape and peak value of the final rotational distribution.[11] Principally we shall be concerned with changes occurring within benzene on collision with various partners and thus the diagrams are plotted in the form of *momentum*–AM plots. A full description of the construction and use of these figures is contained in recent reviews.[7,8] This representation displays energy and AM conservation relations for each transition from initial to final $|v,J\rangle$ states. The figures thus make clear the nature of the constraints that operate on each transition. Plots are of momentum versus rotational AM for the *threshold* or channel-opening condition of (a) linear-to-rotational AM conversion and (b) kinetic to rotational energy conversion. The first of these is

$$\Delta J = \mu v_r b_n^{\max}, \tag{1}$$

where ΔJ=change of rotational AM on collision, μ=collision reduced mass, v_r is velocity of relative motion, and $b_n^{\max}$ is the maximum torque arm available to convert linear-to-angular momentum (LM→AM). $b_n^{\max}$ is found from experiment to be half the bond length in a homonuclear diatomic molecule[17,18] and an equivalent distance from the center-of-mass in a heteronuclear species. For *J*-changing collisions of benzene, the torque arm is initially assumed to be the distance from the molecule's center-of-mass to the H atoms. However, we show later that *J*- and *K*-changing collisions may be simulated using an "equivalent rotor," the dimensions of which may be obtained from the moment of inertia of the molecule about the *b* or *c* inertial axes. These are readily calculated from the molecule's rotational constants and give equivalent rotor lengths of 2.18 Å (*b* axis) and 3.1 Å (*c* axis). This procedure is discussed in more detail and justified in Sec. III. As in the case of diatomic molecules, $b_n^{\max}$ values in $p_r - \Delta J$ (or ΔK) plots are one half of these equivalent rotor lengths. Equation (1) (the *A* equation) represents the *unmodified* expression for LM→AM conversion that frequently must be modified to meet energy conservation constraints.

The energy conservation relationship is process dependent. The generic form is $\Delta E = 1/2 \mu v_r^2$ that for the specific case of VRT becomes

$$\Delta J = \sqrt{(J_i + \tfrac{1}{2})^2 - (\hbar \omega \Delta v \pm \tfrac{1}{2}\mu v_r^2)/B} - (J_i + \tfrac{1}{2}). \tag{2}$$

In Eq. (2), ω is the vibrational frequency, Δv the number of vibrational quanta excited or relaxed, and *B* the molecule's rotational constant. Higher order terms are not shown but are routinely included in all computations. Equation (2) is quantum-state specific as well as ensuring overall energy conservation in the collision and is referred to as the *E* equation. The conservation relations may be plotted as $v_r - \Delta J$ or $p_r - \Delta J$ plots. The latter form is used here as the *A* equation for benzene becomes a single, linear plot whatever the collision partner. Note that the *E* plot simply displays the disposition of final molecular quantum states relative to the initial state in terms of relative momentum or velocity.

A. Monatomic collision partners

A and *E* plots for the $6^1 \rightarrow 0^0$ transition in S_1 benzene are shown in Fig. 3(a) for monatomic collision partners with $K_i = K_f = 0$ and $J_i = 0$. VRT here consists of simultaneous vibrational relaxation and rotational excitation and a backward-arching *E*-plot characterizes this form of transition.[11] In VRT the maximum J_f calculated from energy conservation is often considerably larger than that allowed by AM conservation and the full shape of the arch may not be seen. For each ΔJ channel the two relationships specify relative velocities that are allowed or forbidden in terms of energy (*E* plot) or angular momentum (*A* plot), thus delineating, in analogy to the well-known phase diagram, a region that is allowed by both energy and AM conservation for benzene–He collisions [that shaded in Fig. 3(a)]. Figure 3(a) demonstrates that for a given energy difference the equivalent gap in relative momentum terms is a function of collision partner reduced mass. Note that the *A* plot shown in Fig. 3(a) (and in all other $p_r - J_f$ plots) has not been modified to account for energy conservation. In practice, this is achieved by constraining permitted values of $b_n^{\max}$ in Eq. (1).

As Fig. 3(a) illustrates, energy constraints are strongly dependent on J_f and are particularly stringent at low values of J_f. For $J_f \geqslant 12$ when He is the collision partner the LM→AM process is unrestricted by energy conservation. This constraining effect is not readily expressed analytically though it is straightforwardly incorporated into a computational routine. Energy constraints set a maximum on the values of b_n that are permitted in the LM→AM conversion driving the change and as discussed above may be strongly *J* dependent. For each final *J* channel a new maximum b_n must be evaluated, one consistent with energy conservation. In

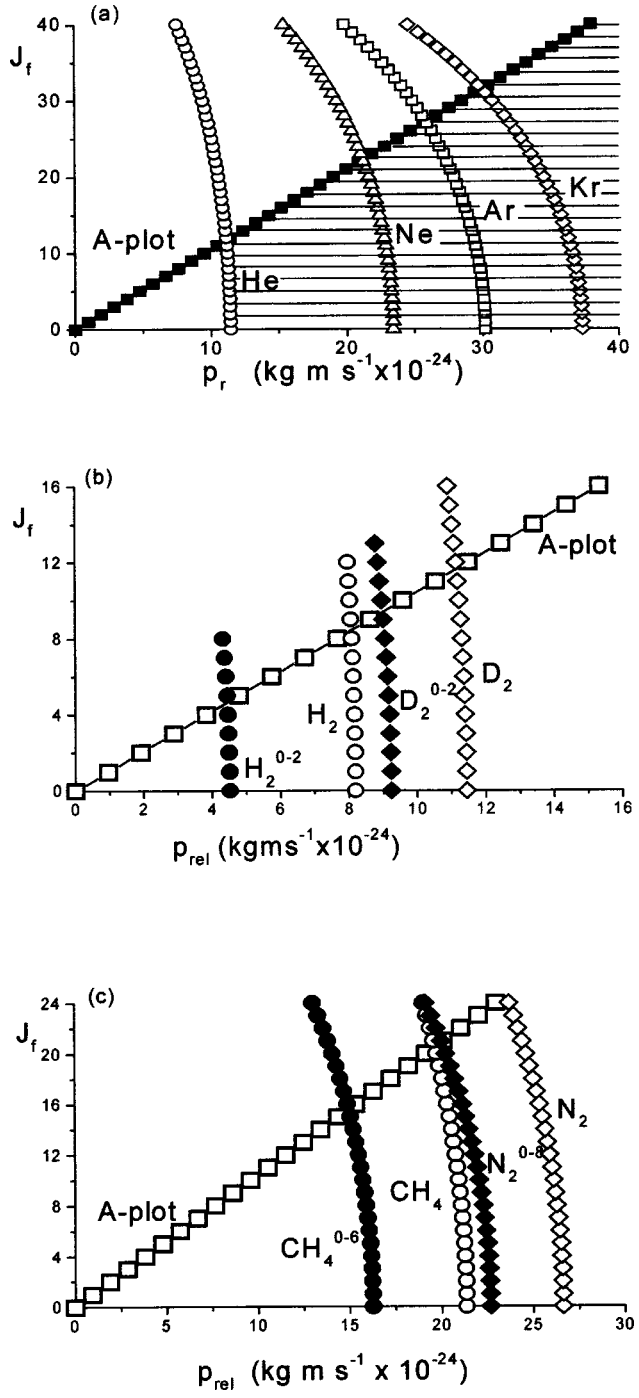

FIG. 3. Momentum–angular momentum plots for $(6^1,0)\rightarrow(0^0,J_f)$ VRT in benzene. Square symbols represent unmodified *A* plots [Eq. (1)] throughout. (a) *E* plots [Eq. (2)] for He, Ne, Ar, and Kr (open symbols). The shaded portion represents the region of momentum–AM space that is allowed by energy and AM conservation for benzene–He. (b) *E* plots are for H_2 (circles) and D_2 (diamonds) collision partners either in their ground states (open symbols) or rotationally excited $0\rightarrow2$ (solid symbols). (c) As for (b) but with N_2 (diamonds) and CH_4 (circles) collision partners. The effect of exciting rotational transitions $0\rightarrow6$ in CH_4 (circles) and $0\rightarrow8$ in N_2 (diamonds) is shown (solid symbols).

terms of the diagrammatic representation this shifts the appropriate point on the *A* plot to the high velocity side of the *E* plot, a process that restricts the velocities contributing to a particular channel. Momentum–AM diagrams may also be constructed for *K*-changing collisions though *K*- and *J*-changing processes are not unambiguously identifiable in the experimental spectra.[4,5] In diatomics the *J* value at which *A* and *E* plots intersect is generally a good guide to the peak of final rotational distribution both in VRT[11] and in the vibrational predissociation of van der Waals molecules.[13] This intersection represents the lowest J_f (or K_f) for which all b_n up to the maximum available may be used without violating energy conservation and constitutes the most probable exit channel.

The probability of rotational state change falls rapidly with the magnitude of ΔJ,[18,19] an effect that may be masked by energy constraints. In the absence of specific constraints, transitions are most probable for lowest ΔJ and largest $b_n^{\max}$. In the vibrational relaxation a substantial amount of energy must be converted into rotation in order for the deactivation to occur. The larger the energy ''load'' to be disposed of, the greater is the amount of AM that must be generated and there will be limits that, for a given collision partner, will be a function of the molecule's moment of inertia. For $6^1\rightarrow0^0$ in benzene Fig. 3(a) predicts the most probable exit channel (for $K_i=K_f=0$) to be $J_f=12$ in collision with He. This value increases markedly with partner mass, becoming 22, 27, and 32 units for Ne, Ar, and Kr, respectively. These represent substantial AM changes. Experiment indicates that the probability $6^1\rightarrow0^0$ VRT is very low for atomic collision partners, rationalized by Waclawik and Lawrance[4] in terms of the difficulty in disposing of large amounts of AM. Their data indicate a very small peak with extensive rotational structure in the appropriate region for $6^1\rightarrow0^0$ VRT when He is the partner (Fig. 2) but the signal was too low to extract a rate constant.[4] Thus we conclude that in benzene, $J_f=12$ represents the upper limit of attainable AM in disposing of 522 cm^{-1} with a collision partner of mass=4 amu. The contribution from relative motion here is very small. The values $J_f=22$, 27, and 32 evidently are *not* attainable for Ne, Ar, and Xe, respectively, no signal being observed with these species and we conclude that these AM changes are too large to have measurable probability.

B. Diatomic collision partners

The dynamical behavior described above changes markedly when the collision partner is a diatomic molecule. Part of the energy liberated may excite rotation and/or vibration in the partner species, thus reducing the energy load to be disposed of by the vibrationally excited molecule. Furthermore, the value of $b_n^{\max}$ may be *increased* since there is an interaction involving two torque arms.[20] The influence of the first of these, i.e., energy load reduction, is readily incorporated into p_r-J_f diagrams. Examples when H_2 and D_2 are collision partners are shown in Fig. 3(b) where the *E* relation assumes no partner rotational excitation and also when the $0\rightarrow2$ rotational transition in H_2 or D_2 is excited by collision. In the former case the diatomics are treated as ''atoms'' of mass 2 and 4 amu, respectively. For H_2, peak J_f is lower than for He but a marked reduction is predicted if the transition $0\rightarrow2$ is excited in H_2. This represents the smallest allowed rotational AM change in H_2 and has highest probability of any rotational transition in this species. Some 70%

of the available VRT energy is absorbed, leaving just 159 cm^{-1} to be disposed of. The effect of this is quantified by incorporating this adjusted ΔE into Eq. (2), leading to the E curve shown in Fig. 3(b). The required benzene AM change is much reduced with the peak predicted to shift from $J_f = 8$ to 4.

In contrast, excitation of 0–2 in D_2 is much less advantageous in energy-shedding terms. The transition energy is 182 cm^{-1}, leaving 340 cm^{-1} to be disposed of as benzene rotation. The benzene peak is predicted around $J_f = 9$ when $0 \rightarrow 2$ rotational excitation of D_2 occurs compared to $J_f = 12$ with no collision partner excitation. (Recall from the benzene–He example that $J = 12$ is the limit of AM disposal for mass 4 amu partners.) This enhances the probability of the $6^1 \rightarrow 0^0$ transition as a result of the lowered AM requirement and there will be additional assistance from the increased torque arm as discussed above. The $0 \rightarrow 2$ transition in D_2 has been illustrated for purposes of direct comparison with H_2. The small reduction in peak J_f predicted and the experimental observation that D_2 causes significant transfer to 0^0, suggest that this may not be the most favorable process. p-D_2 can undergo $1 \rightarrow 3$ excitation and, although at 33% it is the minor constituent of n-D_2, some 60% of the $6^1 \rightarrow 0^0$ transition energy may be deposited in this excitation. The $1 \rightarrow 3$ transition was not included in the $p_r - J_f$ diagram of Fig. 3(b) for clarity but was included in quantitative calculations on benzene–D_2 to be described in Sec. IV.

C. Polyatomic collision partners

The interpretation outlined above for H_2 and D_2 may be extended to other collision partners studied by Waclawik and Lawrance and $p_r - J_f$ diagrams may be used to identify the mechanisms operating in species for which more than one transition is possible. This is illustrated for CH_4 and N_2 which would have to undergo substantial J changes to absorb a significant fraction of the $6^1 \rightarrow 0^0$ transition. Figure 3(c) shows E plots with these partners *not* excited on collision and also when ΔJ transitions $0 \rightarrow 6$ in CH_4 and $0 \rightarrow 8$ in N_2 have occurred. Note that these are illustrative of an effect rather than representing optimum absorption of energy or highest probability. Without partner excitation the benzene rotational AM load is high and evidence from the rare gas partners indicates $6^1 \rightarrow 0^0$ VRT is unlikely without assistance via collision partner excitation. However, even with partner ΔJ transitions, the AM to be disposed on relaxation remains high and 0^0 benzene is likely to be rotationally excited. The average J_f is likely to be higher for N_2 than for CH_4 and therefore CH_4 should be more efficient at relaxing 6^1 benzene, as observed. However, the suggestion that rotational excitation should be higher for N_2 than for CH_4 is contrary to observation. Analysis of 0^0 rotational contours gave a $T_{rot} = 55\,K$ for N_2, corresponding to an average $J_f = 18$, whereas J_f is predicted at ~20–21 from the AM plot. Note that AM plots assume $J_i = 0$ in 6^1, whereas the experimental J_i will be higher than this. To match the observed benzene rotational excitation N_2 must undergo substantial changes in J. (Note that under experimental conditions the average J_i for N_2 is ~3, and the $\Delta J = 8$ transition 3–11 would absorb ~100 cm^{-1} more energy than the 0–8 transition illustrated here.) In contrast, the average J_f observed for 0^0 benzene with CH_4 as the partner is 23.[5] Comparison with the AM plots suggests that CH_4 undergoes only small rotational changes. This is investigated further in Sec. IV.

Why then is transfer with CH_4 so efficient? We noted above that a second effect with *molecular* partners is that b_n^{max} may be enhanced by using the torque arm available in the collision partner. CH_4 is advantaged in this mechanism by virtue of possessing four equal length torque arms and hence the generation of CH_4 rotation is less dependent on collision stereochemistry than N_2. Data for other partners suggest that this factor may be quite significant. The branching ratio for $6^1 \rightarrow 0^0$ VRT with cyclo-propane is larger than for C_2H_2 and N_2 despite C_3H_6 having the smallest rotational constant of these three species. Cyclo-propane has three equivalent torque arms, each of which is considerably longer than those of the other species involved and relaxes vibrationally excited benzene quite efficiently.[5] Furthermore, being quite heavy its velocity relative to benzene will be the smallest of the di- and polyatomic collision partners in the series, lengthening the interaction time. This analysis suggests that the future refinement of this approach would incorporate effective torque arms appropriate for the different collision partners.

III. QUANTITATIVE ANALYSIS; AN EQUIVALENT ROTOR MODEL

The kinematic principles described above provide the basis of a rapid, accurate computational routine for predicting collision-induced processes in diatomic molecules.[7,8] Extending this approach to polyatomics represents a challenge due to the complexity of rotational motion in species containing more than one inertial axis. In the general case collisions involving a symmetric rotor change both J and K quantum numbers. Simplified models of simultaneous J- and K-changing collisions are hampered by the difficulty of finding an analytic function to represent the shape of the hard wall in molecules other than the linear rotor. Furthermore there are relatively few experimental or theoretical data for inter- as well as intra-K stack transitions. Cross sections for J-, K_a- and K_c-changing collisions are available for the asymmetric rotor NH_2,[6,21] but few others exist. Frequently however collision-induced RT and VRT in polyatomics consists of excitation or relaxation directed principally along just one of the inertial axis, giving sets of ΔJ *or* ΔK cross sections or probabilities. A more limited first objective in treating this complex topic therefore might be to develop simplified semiquantitative models that predict transition probabilities *along* inertial axes within the molecule and to leave until later the more difficult problem of axis-switching collisions. This is the approach adopted here where J- and K-changing transitions are addressed separately. We first describe the model and then use it to calculate ΔJ and ΔK distributions for systems in which experimental data are available.

A critical parameter in the AM model for diatomic collisions is the maximum available torque-arm. This quantity is half the molecule's bond length in a homonuclear diatomic or the distance from the molecule's center-of-mass in a het-

eronuclear species.[7,8] A second important parameter is the molecule's moment of inertia. A hard shell ellipsoid based on the diatomic bond length and having the appropriate atomic masses and rotational constant has proved to be very successful in quantitative calculations on diatomics. For our simplified model where *J*- and *K*-changing transitions are addressed separately, interest is limited to processes occurring about one well-defined molecular axis. We introduce the notion of an ''equivalent rotor,'' i.e., a linear rotor having the moment of inertia, bond length, and rotational constant of the polyatomic along the molecular inertial axis of interest. Rotations of this rotor give rise to *J* or *K* change. This approach builds on the principles that successfully describe collisional transfer in diatomic molecules.

To illustrate this idea, consider *J*-changing processes in benzene. Here the appropriate equivalent rotor has mass 78 amu (i.e., $\mu = 32.37 \times 10^{-27}$ kg) and rotational constant equal to the *B* value of benzene (0.18105 cm^{-1}). For the case of ΔK transitions, the equivalent rotor also has mass 78 amu but now the rotational constant is set at $(C\text{-}B) = 0.0905\,cm^{-1}$. The choice of equivalent rotor bond length is not straightforward since it will be a function of the point of impact of the collision partner on the benzene molecule. In the absence of fully resolved data the value of b_n^{max} is not known and furthermore *J* and *K* transitions are not separately identified in the data. In such circumstances we suggest that, unless there are data indicating an alternative value, a conservative approach be adopted in which the equivalent rotor bond length is evaluated from the mass and moment of inertia from the expression $I = \mu r^2$, where *I* is obtained from the appropriate rotational constant. Note that the appropriate mass to be used in such a calculation depends on the location of the inertial axis in the molecular frame. Here again we use a conservative approach and comment later on alternatives, highlighting the need for fully resolved data. In benzene, the equivalent rotor bond lengths are 2.18 and 3.1 Å for rotations about the *b* and *c* axes, respectively. The equivalent rotor approach reduces *J*- or *K*-changing collisions in a polyatomic to angular momentum changes in the ''equivalent'' diatomic. The probability of LM→AM conversion is calculated using the dimensions of the molecule of interest or via the method described above with energy constraints imposed by the *J* or *K* quantum levels. The method is transparent and parallels techniques used in the field of diatomic collision and reaction dynamics. However calculations based on such a simplified model must be tested against known data before being used more widely.

IV. CALCULATIONS USING THE EQUIVALENT ROTOR MODEL

Experimental data that would test the equivalent rotor model are relatively sparse, given that a reasonable number of data points are required to evaluate the method. Data from two experiments are used here, the first being the extensive *K*-changing RT and VRT cross sections for glyoxal–Ne collisions reported by Clegg *et al.*[16] the second being *J*-changing RT rate constants in acetylene–He encounters of Henton *et al.*[22] Here equivalent rotor model predictions are compared with experiment and the method then used to predict rotational distributions for $6^1 \rightarrow 0^0$ VRT transfer for benzene. VRT data in benzene are less well resolved than those for glyoxal or acetylene but despite this, valuable insights are obtained. The method of calculating final *J* or *K* distributions is that recently described for diatomic molecules[7,8,11] and found to accurately reproduce experimental data.[11]

A. Glyoxal

Analysis of rotational contours in the experimental data for glyoxal indicates that *K*-changing collisions dominate inelastic processes.[16] The equivalent rotor for glyoxal was determined as in Sec. III, though in this case the ''bond length'' was calculated from molecular dimensions, giving a value of 2.7 Å. This approach is appropriate because an AM model fit to experimental RT data by Clegg and Parmenter[23] yields $b_n^{max} = 1.35$ Å. (For this molecule the equivalent rotor bond length evaluated from the rotational constant is very close to that calculated from the molecular dimensions). Figures 4(a) and 4(b) show experimental data on glyoxal–Ne[16] together with the results of equivalent rotor calculations for RT and for VRT. Calculated data were normalized to the $K_f = 3$ probability. Agreement between experiment and model predictions is good. The initial *J* value is unknown and as Clegg *et al.* report $J_i \leqslant 10$, we assume initial state $(J_i, K_i) = (10,0)$. VRT here involves excitation both of vibration and of rotation unlike the case of benzene relaxation. VRT in this model requires no separate mechanism for vibrational state change.[11] Transitions to the new state require velocities sufficient to overcome the momentum ''barrier'' that is apparent in the velocity–AM plot and enters the calculation as an energy constraint.[11]

Figures 4(a) and 4(b) demonstrate that both RT and VRT processes in glyoxal are predicted with quite reasonable accuracy. Experimental uncertainties are not reproduced here, but very few calculated points lie outside the experimental error bars.[16] The level of agreement obtained is quite encouraging, particularly since the data reported by these authors are the most extensive collision-induced cross sections available for a polyatomic molecule. Use of an equivalent rotor bond length also gives good results.

B. Acetylene

For a linear rotor such as acetylene a pseudodiatomic having the actual molecular length (i.e., 3.32 Å) is likely to represent the molecular dynamics quite accurately. Henton *et al.*[22] performed hard shape calculations for C_2H_2–He/Ar/H_2 similar to those described here using potential energy surface data for the ellipse dimensions. The initial rotor state chosen for comparison is $J_i = 10$ thus both relaxation and excitation occur. Experimental and calculated data are shown in Fig. 4(c) where agreement is seen to be good. This also was found by Henton *et al.*[22] and is not wholly unexpected since the method is very successful in diatomics. However this example constitutes a valuable test of this approach in which kinematic properties take precedent over those related to the intermolecular potential. In this species the equivalent rotor bond length cal culated from the *B* value is markedly less than that evaluated from the molecular dimensions. Calculations using this reduced value give reason-

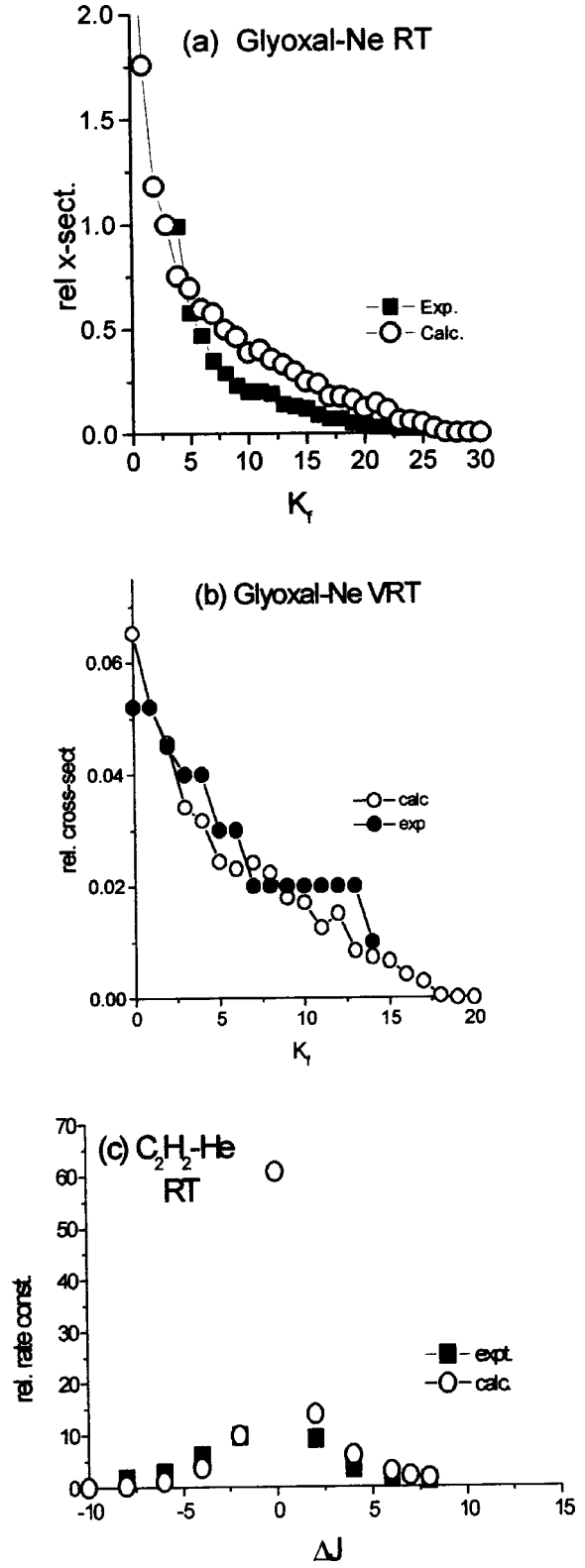

FIG. 4. (a) Rotational $(J,0)\rightarrow(J,K_f)$ and (b) vibration–rotation $0^0(J,0)\rightarrow 7^1(J,K)$ transfer in glyoxal–Ne collisions. Filled symbols represent experimental data (Ref. 16) and open circles are those calculated by the equivalent rotor method. (c) Experimental (Ref. 26) (filled squares) and calculated (open circles) relative rate constants for RT from $J_i=10$ in C_2H_2–He collisions.

able agreement with experimental data however and, together with the calculations of Henton *et al.*,[22] implies that a more extensive data set would be helpful in determining equivalent rotor dimensions.

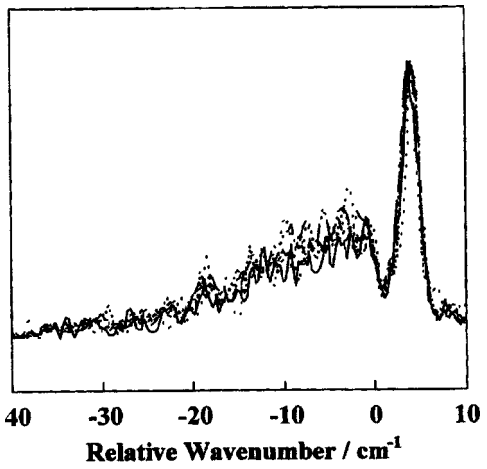

FIG. 5. High resolution (1 cm^{-1}) dispersed fluorescence spectrum of the 6_1^0 band of benzene obtained in a benzene–CH_4 expansion following excitation of six different initial rotational distributions within 6^1.

C. $6^1\rightarrow 0^0$ transfer in benzene

Momentum-based constraints strongly influence events that involve the release of energy such as the $6^1\rightarrow 0^0$ vibrational relaxation in benzene. This constitutes a subtly different process to the rotational or simultaneous vibration–rotational *excitation* in acetylene and glyoxal since now vibrational relaxation accompanies rotational excitation. The most intense transitions will be to those $(0^0 J_f)$ channels that most efficiently dispose of the available energy into angular momentum.[11] Here we calculate the probability that impulse from the excited v_6 vibration will be converted into rotational AM of the target molecule. The equivalent rotor method was used as previously described with the effect of energy transfer into partner rotation simulated by reducing the 522 cm^{-1} of released energy by the amount given up to the partner. The most efficient means of reducing energy load in general is through collision partner *vibration* and experiment indicates that polyatomic collision partners having vibrational modes <522 cm^{-1} strongly enhance $6^1\rightarrow 0^0$ VRT,[24] but none of the partners considered here has modes of sufficiently low energy for $V\rightarrow V$ transfer. *J*- and *K*-state distributions were calculated for benzene–H_2, –D_2, and –CH_4 and compared to data from high-resolution experiments[5] of which Fig. 5 is a representative.

Before describing the results of the calculations we summarize the relevant experimental findings of Waclawik and Lawrance.[4] (i) Some rotational relaxation is evident within the 6^1 and 0^0 levels, particularly for H_2, but this does not affect the nascent 0^0 rotational distributions on the experimental timescale. (ii) The experiment excites initial rotational states in 6^1, with $J_i=4-15$. The 0^0 contours are similar for each laser detuning (i.e., J_iK_i range) and so the 0^0 contours were averaged over all initial distributions prior to fitting. (iii) Boltzmann fits to the 0^0 contours yield nascent $T_{\mathrm{rot}}=19$, 41, and 93 K (average $J_f=10.5$, 15.7, and 23.8) for H_2, D_2, and CH_4, respectively. (Fits were used by Waclawik and Lawrance to estimate average J_f within 0^0 and the values should be viewed as indicative rather than absolute.) The distributions drop more slowly at high *J* than they rise at low *J* and so the average is somewhat higher than

the J value at the distribution maximum. (iv) Calculation of the 0^0 emission contours assuming an exponential decay in ΔJ and ΔK suggest that the K state distribution is very broad when CH_4 is the partner.

The benzene equivalent rotors used in J- or K-changing calculations were described earlier. Calculations were performed for relaxation from 6^1, $J_i = 4$, 7, 10, 12, 15 averaging the 0^0 J_f distributions over J_i with equal weight. All allowed *collision partner* rotational excitations were considered and a representative selection of calculated distributions is shown in Fig. 6. H_2 has only one allowed excitation, the $0 \rightarrow 2$ rotational in p-H_2. With D_2 both $0 \rightarrow 2$ (o-D_2) and $1 \rightarrow 3$ (p-D_2) may occur. In CH_4, rotational excitations $0 \rightarrow 2$, $0 \rightarrow 4$, $0 \rightarrow 6$, and $0 \rightarrow 8$ were included and both J- and K-changing collisions were investigated. These calculations yield information on likely transitions in the collision partner as discussed below. Figure 6(a) shows J_f distributions predicted in the 0^0 level following collision with H_2, D_2, and CH_4. $0 \rightarrow 2$ rotational excitation was assumed in each partner and thus varying amounts of the 522 cm^{-1} energy have been shed. A broad and rather lumpy profile results in which peaks associated with the five J_i states are often discernible. Experimental 0^0 rotational contours are similar for all initial 6^1 J, K distributions[5] and will contain contributions from all pathways, not just those involving $J = 0 \rightarrow 2$ in the collision partner, the individual contributions being unknown. For H_2, where the final distributions are most sensitive to the J_i distribution, $V \rightarrow T$ transfer is a likely contributor to $6^1 \rightarrow 0^0$ relaxation and this will smear the final J distribution.

Calculated distributions are compared in Fig. 6(b) with the thermal distributions found by Waclawik and Lawrance to fit observed rotational contours. The J_f distributions were determined by summing over K state populations. Comparison of Figs. 6(a) to 6(b) shows that the J_f distributions extracted from experiment are remarkably similar to those predicted by the equivalent rotor calculation. A Gaussian fit to calculated H_2 data yields $J_f^{\max} = 10$ and that from the thermal distribution [Fig. 6(b)] is $J_f = 9$ for H_2. Given the approximations involved, this represents satisfactory agreement with experiment. In the absence of collision partner excitation the distribution for C_6H_6–H_2 peaks at $J_f = 13$. The calculated distribution for C_6H_6–D_2 also assumes $0 \rightarrow 2$ excitation in D_2, the lowest energy transition in the major (67%) component (o-D_2). The peak is at $J_f = 12$, compared with a value of 13 for the thermal distribution. The transition $1 \rightarrow 3$ is feasible in p-D_2 and may represent a favored route since a greater proportion of the $6^1 \rightarrow 0^0$ VRT energy can be disposed of. However for this case the rotational distribution curve peaks between $J_f = 10$ and 11. Thus the calculated distributions in conjunction with experiment, suggest excitation of the 0–2 transition in o-D_2 is likely to dominate the deactivation process.

Figure 6(a) also displays the J_f distribution assuming the $0 \rightarrow 2$ rotational transition in CH_4. The benzene 0^0 rotational distribution peak moves steadily to lower J_f as the proportion of disposable energy used in partner rotation is increased. Transitions $0 \rightarrow 2$ and $0 \rightarrow 4$ in CH_4 differ little in energy and the benzene J_f distributions for these two are rather similar. The probability of $0 \rightarrow 2$ is expected to be higher than of $0 \rightarrow 4$. The predicted distribution for $0 \rightarrow 2$ is broad and a Gaussian fit peaks at $J_f = 21$. The thermal distribution extracted from experiment is also broad and peaks $\sim J_f = 21$–22. This suggests that the $0 \rightarrow 6$ and $0 \rightarrow 8$ CH_4 excitations are unlikely since these result in benzene J_f peaks at 17 and 13, respectively. Thus, on the grounds of fit to experiment and transition probability, the $0 \rightarrow 2$ excitation in CH_4 is the most likely process accompanying $6^1 \rightarrow 0^0$ VRT in benzene. The extent to which collision partner rotation aids or hinders overall AM balance may also be a factor and will potentially restrict some collision partner rotational channels, an effect discussed in greater detail by Waclawik and Lawrance.[4] Analysis of high resolution C_6H_6–CH_4 data[5] suggests that K-changing processes are important for this pair and Fig. 6(c) shows predicted K_f state distributions when the $6^1 \rightarrow 0^0$ relaxation occurs exclusively by K-changing collisions from the $(0,K_i)$ level of 6^1 benzene. K_f distributions were calculated for $K_i = 4$, 7, 10, 12, and 15 for each of the collision partner rotational excitations $0 \rightarrow 2$, $0 \rightarrow 4$, $0 \rightarrow 6$, and $0 \rightarrow 8$. The figure illustrates the effect referred to above in that the distributions shift markedly to lower values of K_f as excitation within the collision partner increases.

V. DISCUSSION AND CONCLUSIONS

A. Collision partner dependence of vibrational relaxation in S_1 benzene

We have described qualitative and quantitative methods for analyzing collision-induced rotational and vibration–rotation change in polyatomic molecules, illustrated with special reference to the $6^1 \rightarrow 0^0$ transition in benzene. The analysis supports and quantifies that of Waclawik and Lawrance[4] on the manner in which collision partners influence this relaxation rate. It is not essential to have state-to-state data or full rotational resolution of product states to achieve insight into the factors controlling VRT in polyatomics. A useful overview is gained through the use of momentum–AM diagrams which illustrate the manner in which released energy may be disposed into rotational excitation of benzene. They also show the energy and angular momentum constraints that operate on product rotational channels and identify those rotational states on which these constraints are lifted. The lowest J_f of this latter group frequently provides the principal exit channel for the relaxation.

Graphical methods illustrate how the AM ''load'' is reduced when the collision partner absorbs some fraction of the energy released. For the collision partners considered here this occurs by partner rotation. The load reduction is likely to be very effective when collision partner *vibration* is excited. Recent work[24] reveals that the $6^1 \rightarrow 0^0$ transition in benzene becomes the dominant relaxation pathway when partner vibrational excitation is feasible, consistent with our expectations. H_2 is a very efficient promoter of VRT since over 70% of the 522 cm^{-1} released in the $6^1 \rightarrow 0^0$ transition may be disposed into $0 \rightarrow 2$ rotational excitation of H_2. D_2 is reasonably effective with a smaller fraction of load shed on exciting $0 \rightarrow 2$ in the diatomic. Momentum–AM diagrams allow these effects to be quantified, showing the reduced ben-

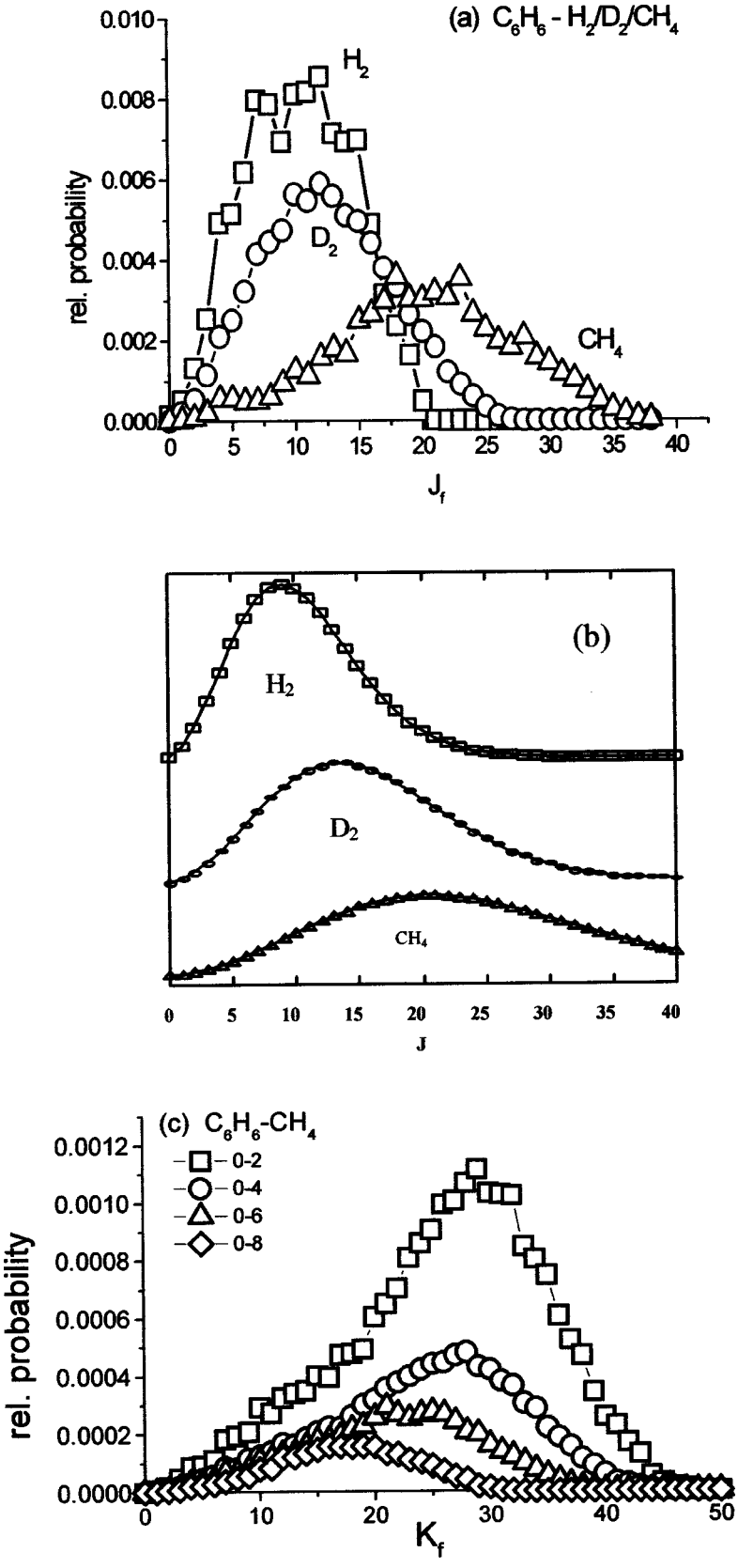

FIG. 6. (a) Calculated J_f distribution following $(6^1,0) \rightarrow (0^0,J_f)$ VRT by H_2 (squares), D_2 (circles), and CH_4 (triangles). Each distribution is an average of $J_i=4$, 7, 10, 12, and 15. Rotational excitation $0\rightarrow2$ is assumed in each collision partner. (b) Experimental J_f distribution following $(6^1,0)\rightarrow(0^0,J_f)$ VRT by H_2 (squares), D_2 (circles), and CH_4 (triangles). J_f is obtained from the thermal distributions that best fit averaged experimental 6_1^0 rotational contours summed over K state populations for a particular J. (c) Calculated K_f distribution for $6^1 \rightarrow 0^0$ VRT in benzene–CH_4 assuming $0\rightarrow2$ (squares), $0\rightarrow4$ (circles), $0\rightarrow6$ (triangles), and $0\rightarrow8$ (diamonds) rotational excitation in CH_4. Each distribution represents an average of $K_i=4$, 7, 10, 12, 15.

zene rotation requirement that accompanies the ''rotationally assisted'' VRT process. When CH_4 and N_2 are the collision partners the load-shedding efficiency is much reduced since large ΔJ transitions must occur within these species to absorb a reasonable fraction of the $6^1\rightarrow0^0$ transition energy and the probability of transition drops rapidly as ΔJ increases. However, a molecule such as CH_4 has enhanced efficiency since it may present any one of its four equivalent C–H torque arms to convert the vibrational impulse into rotation. Cyclopropane is also advantaged in this respect and

has a longer torque arm than other species considered here. The branching ratios and rotational temperatures for $6^1 \rightarrow 0^0$ deactivation reported by Waclawik and Lawrance[3] for a range of collisional partners may be rationalized using these arguments and information from momentum–AM diagrams.

B. The equivalent rotor model

The equivalent rotor model assumes that the critical parameters governing state change in polyatomics are those that determine collision outcomes in diatomic molecules where key molecular factors are bond length and moment of inertia.[7,8] For transitions generating rotational AM along a specific molecular axis the polyatomic is simulated by an ''equivalent diatomic'' whose mass, rotational constant, and length are determined from the shape and size of the polyatomic molecule at 90° to that axis. The model is tested by comparing predicted RT and VRT K_f distributions in glyoxal and J_f distributions from RT experiments on acetylene with those obtained experimentally. The accuracy of the calculations is encouraging, indicating that the method is a useful first attempt at the difficult task of predicting the collision properties of polyatomic molecules. No attempt is made to extend the method to axis-switching transitions. In the absence of fully resolved data on benzene equivalent rotor bond lengths are estimated from moments of inertia of the molecule about specified axes. This avoids the difficulty of estimating torque-arm dimensions from anisotropic structures and could be regarded as erring on the side of caution. The investigation of VRT in this species with full rotational resolution would greatly assist the refinement of this simplified model.

The equivalent rotor method was used to calculate J_f or K_f distributions following $6^1 \rightarrow 0^0$ relaxation by H_2, D_2, and CH_4. Calculations were performed for $J_i = 4$, 7, 10, 12, 15, and $0 \rightarrow 2$ partner rotational excitation was assumed. Good agreement with experimental was obtained. The calculations distinguish shifts in J_f (or K_f) as partner excitation changes, permitting identification of probable rotational transitions in the partner. The benzene rotational shifts may be quite large and study of this hidden process becomes feasible despite the lack of resolution in the target species.

C. Relaxation pathways in polyatomic molecules

The findings of this study may be of wider significance, an obvious parallel being vibrational predissociation of van der Waals molecules[11,25,26] but there are numerous situations throughout chemistry in which large amounts of energy must be disposed of when a molecule changes state. We suggest that the efficiency with which a system converts this energy into rotational and orbital AM greatly influences the probability and speed of the transition. In the $6^1 \rightarrow 0^0$ transition in benzene a controlling factor appears to be the ability of benzene to generate the appropriate amount of rotational AM at the same time as deactivating the v_6 mode. Experiment indicates that, for a given system, there are inherent limits on the amount of energy that may be released in collision-induced VRT and that the process of angular momentum creation sets these limits.

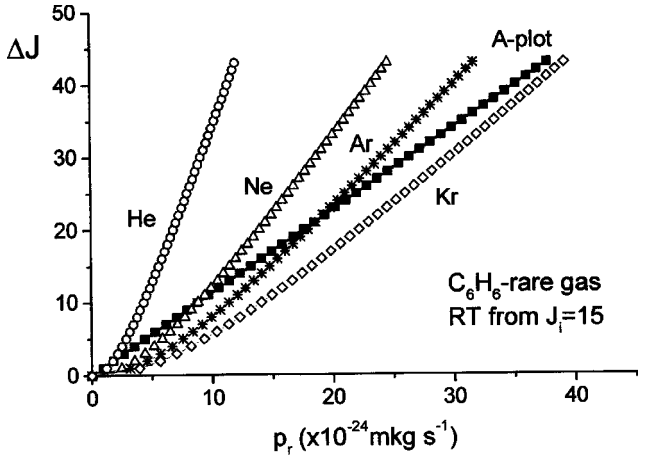

FIG. 7. *A* and *E* plots for benzene–rare gas RT to illustrate the increased energy constraints as partner mass increases. The figure represents RT from $J_i = 15$ of S_1 benzene.

Similar behavior has been observed in the vibrational relaxation of diatomic molecules. Whereas early work focused principally on molecules in low vibrational levels,[27] the development of stimulated emission pumping[28] and of overtone pumping[29] has allowed investigation of species in highly excited vibrational states.[2] Light collision partners are much more effective quenchers of large vibrational energy gaps than heavy species for molecules in low and high vibrational states. Single quantum relaxation often dominates, even when the diatomic is highly excited and evidently there are limits to the amount of energy that may be released on collision however much is contained initially within vibrational modes. Yang *et al.*[30] observed that the $v = 22$ level in (^2X)NO is not relaxed by Ar and He but the VRT rate constant becomes large when H_2 is the collision partner. Experiments of Lester and co-workers[25,26] on vibrational predissociation of van der Waals molecules demonstrate that dissociation lifetimes are reduced by many orders of magnitude when a substantial fraction of the energy of dissociation is shed as partner vibration or rotation. At the same time the angular momentum load is much reduced as seen in the resulting rotational distributions.[26]

Significant questions arise from these observations. (i) Why are lightest collision partners most effective in bridging large energy gaps? Heavy partners that carry substantial momentum might be expected to be more effective than light species. (ii) What limits the amount of energy that may be released in a relaxation process? No obvious explanation exists in terms of, say, energy conservation. (iii) Why is vibrational relaxation in polyatomics so mode specific? The *in*sensitivity of inelastic cross sections to kinematic factors was addressed by Clare *et al.*[31] and Fig. 7 illustrates the origin of this effect in benzene. Energetic constraints are strongly enhanced as collision partner mass increases and at the same time the number of channels subject to these constraints increases dramatically. Figure 7 is constructed for RT in S_1 benzene ($J_i = 15$) and demonstrates that although heavy partners bring greater momentum to the collision, the number of allowed trajectories for a given channel is diminished by energy conservation, and affects more J_f channels as reduced

mass increases. This is a feature of diatomic RT cross sections and increases strongly with J_i. Thus light collision partners will generally improve the efficiency of processes that take place through the generation of rotational AM.[31]

What does experiment tell us regarding the remaining questions from the preceding paragraph? Benzene data, the analysis of Waclawik and Lawrance,[4,5] and the theory presented here suggest a general principle in molecular collision dynamics for processes that involve the liberation of energy. Whether or not the process occurs and, if it should occur, its rate constant or cross section is governed by the ability of the molecule and collision partner to convert impulse into rotational AM. Molecules vary considerably in their ability to convert momentum change into rotation though the controlling factors are now understood.[7,8] The $6^1 \rightarrow 0^0$ transition in benzene is of particular interest since this relaxation is just observable for He (Fig. 2) but no signal is seen when heavier rare gases are collision partners. This transition becomes measurable, though still small, for He when benzene-d_6 is the target species[32] where now the $6^1 \rightarrow 0^0$ energy gap is 498 cm^{-1}. This 24 cm^{-1} reduction compared to C_6H_6 lowers the ΔJ (and/or ΔK) required to absorb the released energy and there is a small increase in probability. The effect by which light gases enhance transfer to energy levels having large energy separations is well established, having been observed in benzene-d_6[33] and also in *p*-difluorobenzene.[34] What then is the cause of these limitations on the energy that may be liberated? Clearly this is an effect of some significance. In the $6^1 \rightarrow 0^0$ transition in benzene, all the available energy within the S_1 excited electronic state is released but in numerous other instances this is not the case and strict limits appear to exist on the de-excitations that may occur despite there being high levels of excitation remaining within a specific electronic state or within the molecule.

Why is *all* excess energy not released in collision-induced de-excitation and transition to the lowest level the norm in all collision-induced processes of molecules in excited vibrational and/or electronic states whatever the magnitude of the energy gap to be overcome?[35] This appears very rarely to be the case. The work described here suggests a possible, relatively simple explanation for this phenomenon. In the vibrational de-excitation process there is conversion of the impulse generated on contact between collision partner and the vibrationally excited benzene molecule into benzene rotation, orbital angular momentum of the collision pair, and, where feasible, internal excitation of the collision partner. The analysis here suggests that $6^1 \rightarrow 0^0$ relaxation occurs most effectively when the majority of this impulse becomes benzene rotation and hence there are similarities to the well-known kinematic limit of the atom–diatom chemical reaction[36] when all reactant orbital AM becomes product rotation. The *J* and/or *K* change that must be induced on relaxation increases as the energy gap increases and the dependence on reduced mass was discussed earlier. However, it is well known that, in the absence of specific energetic constraints, the probability of AM change falls rapidly as ΔJ increases[37] so that large ΔJ transitions have very low probability.

Thus, for a given molecule there will be a natural limit to the energy gap that may be spanned in a relaxation process and this is reached when the *J or K* change that is a necessary accompaniment to the energy release has become too large to have significant probability. Critical factors in this are the moment(s) of inertia of the molecule and the length of available torque arm(s), i.e., $b_n^{\max}$. Alleviation of this restriction may be achieved by choosing a light monatomic collision partner or, alternatively, a partner capable of absorbing a substantial fraction of the released energy preferably in the form of vibration since in this way no additional AM is generated. The high selectivity of pathways in vibrational transfer in polyatomic molecules[2,3] may be a manifestation of this same principle though with some additional conditions. In vibrational relaxation, the nuclear motions on collision must be such that the required amount of rotational angular momentum is generated and *simultaneous* vibrational state change occurs. These conditions place strong constraints on the forms of the vibrational modes undergoing deactivation and excitation, on the direction of collision partner approach and on the efficiency with which a molecule can convert impulse (i.e., orbital or linear momentum) into molecular rotation. It is observed, for example, that the transfer $6^1 \rightarrow 4^1$ in benzene does not occur even though it is energetically favored and other $|\Delta v| = 2$ transfers are observed.[27] The case of glyoxal provides a particularly vivid example where rotation about the *a* axis accompanies activation or deactivation of ν_7, a CHO–CHO torsional mode.[16] Here the torque arm for linear-to-angular momentum conversion leading to *K*-axis excitation is substantial and thus the needs of vibration and rotation are simultaneously satisfied by a collision that impacts, for example, on one of the H atoms. In the case of vibrational excitation the ability to excite simultaneous rotation greatly adds to the overall VT cross section since this latter quantity is simply the sum of the rotational transitions between the two manifolds.[11] Thus in large molecules where many vibrational modes exist, the nuclear motion of the vibrational mode undergoing deactivation must be such as to provide impulse that will generate molecular rotation about the *a* or the *c* axis on impact with the collision partner. This is likely to be a stringent requirement and hence selectivity among modes for relaxation is expected to be high. However, when all factors are optimized, highly efficient vibrational relaxation would be anticipated.

ACKNOWLEDGMENTS

We thank Professor Charles Parmenter and Dr. Sam Clegg for data on glyoxal prior to publication. M.A.O. wishes to thank the Royal Society for a University Research Fellowship.

[1] A. Schiffman and D. W. Chandler, Int. Rev. Phys. Chem. **14**, 371 (1995).
[2] G. W. Flynn, C. S. Parmenter, and A. M. Wodtke, J. Phys. Chem. **100**, 12817 (1996).
[3] S. A. Rice, J. Phys. Chem. **90**, 3063 (1986).
[4] E. R. Waclawik and W. D. Lawrance, J. Chem. Phys. **102**, 2780 (1995); **109**, 5921 (1998).
[5] E. R. Waclawik and W. D. Lawrance, J. Phys. Chem. A **107**, 10507 (2004).
[6] Z. T. AlWahabi, C. G. Harkin, A. J. McCaffery, and B. J. Whitaker, J. Chem. Soc., Faraday Trans. 2 **85**, 1009 (1989).

[7] A. J. McCaffery and R. J. Marsh, J. Phys. B **34**, R131 (2001).
[8] A. J. McCaffery, Phys. Chem. Chem. Phys. **6**, 1637 (2004).
[9] J. D. Lambert, *Vibrational and Rotational Relaxation in Gases* (Oxford University Press) London, 1977).
[10] D. C. Clary, Chem. Phys. **65**, 247 (1982); A. J. Banks, D. C. Clary, and H. J. Werner, J. Chem. Phys. **84**, 3788 (1986).
[11] R. J. Marsh and A. J. McCaffery, J. Phys. B **36**, 1363 (2003); A. J. McCaffery and R. J. Marsh, J. Phys. Chem. A **104**, 10442 (2000).
[12] A. J. McCaffery and R. J. Marsh, J. Chem. Phys. **115**, 9771 (2001).
[13] A. J. McCaffery and R. J. Marsh, J. Chem. Phys. **117**, 6478 (2002).
[14] K. Truhins, R. J. Marsh, A. J. McCaffery, and T. W. J. Whiteley, J. Chem. Phys. **112**, 5281 (2000); A. J. McCaffery, K. Truhins, and T. W. J. Whiteley, J. Phys. B **31**, 2023 (1998); R. J. Marsh, A. J. McCaffery, and M. A. Osborne, J. Phys. Chem. A **107**, 9511 (2003).
[15] Z. T. Alwahabi, N. A. Besley, A. J. McCaffery, M. A. Osborne, and Z. Rawi, J. Chem. Phys. **102**, 7945 (1995).
[16] S. M. Clegg, A. B. Burrill, and C. S. Parmenter, J. Phys. Chem. A **102**, 8477 (1998).
[17] M. A. Hoffbauer, S. Burdenski, C. F. Giese, and W. R. Gentry, J. Chem. Phys. **78**, 3832 (1983).
[18] M. A. Osborne and A. J. McCaffery, J. Chem. Phys. **101**, 5604 (1994).
[19] A. J. McCaffery, Z. T. AlWahabi, M. A. Osborne, and C. J. Williams, J. Chem. Phys. **98**, 4586 (1993); M. A. Osborne, A. J. Marks, and A. J. McCaffery, J. Phys. Chem. **100**, 3888 (1996).
[20] R. J. Marsh and A. J. McCaffery, Chem. Phys. Lett. **335**, 134 (2001).
[21] F. Linder and R. Wilhelm, J. Chem. Phys. **117**, 4878 (2002); F. Dong, X. Li, M. Zhang, X. Wang, and N. Lou, *ibid.* **111**, 10578 (1999).
[22] S. Henton, M. Islam, S. Gatenby, and I. W. M. Smith, J. Chem. Soc., Faraday Trans. **94**, 3219 (1998).
[23] S. M. Clegg and C. S. Parmenter (unpublished).
[24] E. R. Waclawik and W. D. Lawrance, J. Phys. Chem. A **107**, 10507 (2004).
[25] B. V. Pond and M. I. Lester, J. Chem. Phys. **118**, 2223 (2003).
[26] M. T. Berry, M. R. Brustein, and M. I. Lester, J. Chem. Phys. **92**, 6469 (1990); J. M. Hossenlopp, D. T. Anderson, M. W. Todd, and M. I. Lester, *ibid.* **109**, 10707 (1998); M. D. Marshall, B. V. Pond, S. M. Hopman, and M. I. Lester, *ibid.* **114**, 7001 (2001); M. D. Wheeler, T. Tsiuris, M. I. Lester, and G. Lendvay, *ibid.* **112**, 6590 (2000).
[27] J. T. Yardley, *Introduction to Molecular Energy Transfer* (Academic, New York, 1980).
[28] See for example, X. Yang and A. M. Wodtke, Int. Rev. Phys. Chem. **12**, 123 (1993).
[29] See for example, F. F. Crim, Annu. Rev. Phys. Chem. **35**, 657 (1984).
[30] X. Yang, E. H. Kim, and A. M. Wodtke, J. Chem. Phys. **96**, 5111 (1992).
[31] S. Clare, A. J. Marks, and A. J. McCaffery, J. Phys. Chem. A **104**, 7181 (2000).
[32] R. A. J. Borg, E. R. Waclawik, Mudjijono, and W. D. Lawrance, Chem. Phys. Lett. **218**, 320 (1994).
[33] M. W. Rainbird, B. S. Webb, and A. E. W. Knight, J. Chem. Phys. **88**, 2416 (1988).
[34] D. L. Catlett, Jr. and C. S. Parmenter, J. Phys. Chem. **95**, 2864 (1991); C. J. Pursell and C. S. Parmenter, *ibid.* **97**, 1615 (1993).
[35] K. McKendrick (private communication).
[36] I. R. Elsum and R. G. Gordon, J. Chem. Phys. **76**, 3009 (1982).
[37] T. E. Brunner, N. Smith, A. W. Karp, and D. E. Pritchard, J. Chem. Phys. **74**, 3324 (1981).